Biochimica et Biophysica Acta 1788 (2009) 484–494

Contents lists available at ScienceDirect

Biochimica et Biophysica Acta

journal homepage: www.elsevier.com/locate/bbamem

Probing molecular level interaction of oseltamivir with H5N1-NA and model membranes by molecular docking, multinuclear NMR and DSC methods

Charlotte D'Souza [a], Meena Kanyalkar [a], Mamata Joshi [b], Evans Coutinho [c], Sudha Srivastava [b,*]

[a] Prin K M Kundnani College of Pharmacy, Cuffe Parade, Mumbai-400005, India
[b] National Facility for High Field NMR, Tata Institute of Fundamental Research, Homi Bhabha Road, Mumbai-400005, India
[c] Bombay College of Pharmacy, Kalina, Mumbai-400098, India

ARTICLE INFO

Article history:
Received 17 July 2008
Received in revised form 14 November 2008
Accepted 14 November 2008
Available online 28 November 2008

Keywords:
Neuraminidase
Oseltamivir
Model membrane
Docking
NMR
Differential scanning calorimeter

ABSTRACT

Structure-based drug design has led to the introduction of three drugs — oseltamivir (GS-4104), zanamivir (GG-167) and peramivir (RWJ-270201) which target the enzyme neuraminidase, for treatment of influenza infections. Using comparative docking studies we propose that more potent molecules against neuraminidase can be obtained by appending extra positively charged substituents at the C5 position of the oseltamivir skeleton. This provides an additional interaction with the enzyme and may overcome the problem of resistance encountered with these drugs. To get an insight into the transport and absorption of oseltamivir — the ethyl ester prodrug (GS-4104) as well as its mechanism of action, we have carried out ^{1}H, ^{13}C, ^{31}P NMR, DSC and TEM studies on GS-4104 with model membranes prepared from DMPC/DPPC/POPC. These studies reveal that interactions between GS-4104 and the membrane are both electrostatic (involving H-bonding) and hydrophobic (involving the hydrophobic chain and cyclohexene ring of GS-4104) in nature. The prodrug is seen to increase the fluidity as well as stabilize the bilayer phase of the membrane. This property may be responsible for preventing viral entry into the cells by preventing fusion of the virus outer coat with the cell membrane.

1. Introduction

The danger of the highly pathogenic H5N1 influenza virus is not only its high fatality but also its resistance to commercially available drugs. The influenza virus contains two surface glycoproteins, haemagglutinin (HA) and neuraminidase (NA) [1,2]. HA is responsible for the binding of the virus to the target cells *via* the terminal sialic acid residue in glycoconjugates. In contrast, NA catalyzes the removal of the terminal sialic acid linked to glycoproteins and glycolipids. It has been postulated that NA activity is necessary in the elution of newly formed viruses from infected cells by digesting sialic acid in the HA receptor [3,4]. Because of its essential role in influenza virus replication, and its highly conserved active sites, inhibiting NA can delay the release of progeny virus from the surface of infected cells, thereby suppressing the viral population. NA has therefore become an important target for drug design against influenza viruses.

Studies on DANA (2,3-didehydro-2-deoxy-N-acetylneuraminic acid) [5], a prototype NA inhibitor, which is a sialic acid (endogenous substrate) analogue has lead to drugs like oseltamivir — the ethyl ester prodrug (GS-4104) [6], zanamivir (GG-167) [7] and peramivir (RWJ-270201) [8] (Fig. S1). Zanamivir has poor bioavailability and is therefore administered by inhalation. On the other hand, GS-4104 as the phosphate (Fig. 1a) is the first orally active neuraminidase inhibitor approved for the treatment of both influenza A and B infections [9].

GS-4104 [Ethyl-(3R, 4R, 5S)-(1-ethylpropyloxy)-4-acetamido-5-amino-1-cyclohexene-1-carboxylate)] is an ethyl ester prodrug which is hydrolyzed to the active form oseltamivir carboxylate (GS-4071, Fig. 1b) [10]. GS-4071 has poor oral bioavailability (less than 5% in rats) [11]; on the other hand, the prodrug GS-4104 is considerably more hydrophobic (log P=0.36) than GS-4071 (log P=−2.1). This increased lipophilicity is seen to improve the bioavailability of GS-4071 which ranges from 30 to 60% in various animals species, after oral administration of GS-4104 in its phosphate salt form [12]. The transport of the drug and its absorption through the gastrointestinal tract can be understood by studying the interaction of the prodrug GS-4104 with model membranes prepared from a variety of phospholipids. However, the antiviral activity ensues from the interaction of the parent drug (GS-4071) with the neuraminidase receptor and this aspect can be probed by docking studies of GS-4071 with its receptor.

The H5N1-NA active pocket (binding region) consists of 11 functional residues which participate in the catalytic reaction [13]. The binding region shows four well-conserved binding sites [14]. The positively charged site-1 consists of Arg118, Arg292 and Arg371, which interacts with the carboxylate group of the inhibitors. The negatively charged site-2 consisting of Glu119, Glu227 and Asp151 interacts with

* Corresponding author. Fax: +91 22 22804682.
E-mail address: sudha@tifr.res.in (S. Srivastava).

0005-2736/$ – see front matter © 2008 Elsevier B.V. All rights reserved.
doi:10.1016/j.bbamem.2008.11.014

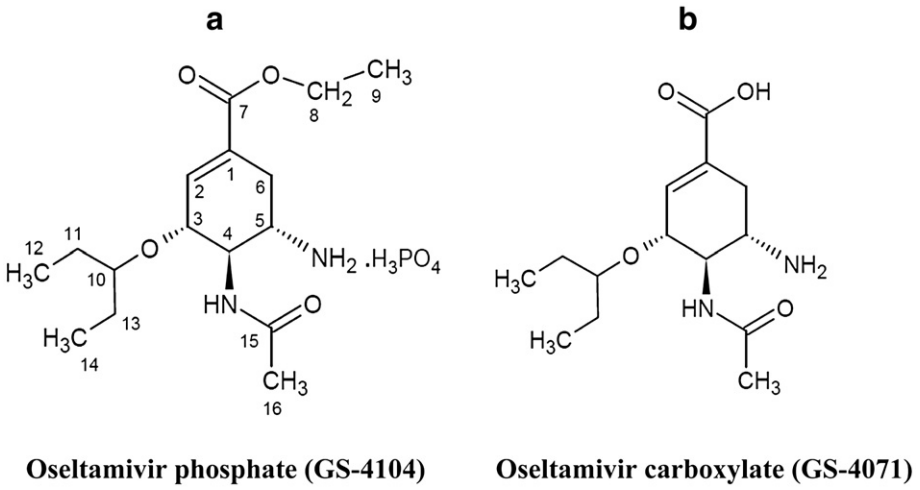

Fig. 1. Molecular structure of (a) oseltamivir phosphate — the ethyl ester prodrug (GS-4104) with atom labels (b) oseltamivir carboxylate (GS-4071).

the guanidino or the amino group of the inhibitors. Site-3 has Ile222 and Tyr178, which accommodates the acetyl group of the inhibitors and site-4 consists of Glu276 and Glu277 which binds to the glycerol part of sialic acid or the hydrophobic part of the inhibitors. Moreover, presence of a 150 loop (residues 147–152), adjacent to the active site leads to the formation of closed and open conformations, enabling binding to the inhibitors [15].

In the present study we have used the approach of molecular docking of GS-4071 to the enzyme H5N1-NA to explore the active site and to provide clues to favorable binding interactions that can be used to modify the existing drugs.

NA inhibitors inhibit the binding of HA and thus its ability to promote attachment and fusion of the cell membrane to the virus [16,17]. By this process it is likely to interfere with cell–cell fusion thus interfering with the virus entry step. In view of this, we have carried out a detailed investigation of GS-4104 (Fig. 1a) with model membranes prepared from DMPC/DPPC/POPC, using nuclear magnetic resonance (NMR) and differential scanning calorimetric (DSC) techniques. The results have been further supported by transmission electron microscopic (TEM) studies. These studies provide detailed information on the effect of the drug on the lipid head group and the conformation and dynamics of the hydrophobic chain [18,19].

The effect of GS-4104 on the phase of the bilayer membrane and its mobility/fluidity may have an implication on membrane fusion and the viral replicative process as indicated in these studies. This knowledge will be used in the future to design some new inhibitors with better activity and hopefully lower viral resistance.

2. Experimental

2.1. Materials

Oseltamivir phosphate (GS-4104) was a gift from Cipla Ltd., India. 1,2-dimyristoyl-*sn*-glycero-3-phosphocholine (DMPC) and 1,2-dipalmitoyl-*sn*-glycero-3-phosphocholine (DPPC) were purchased from Sigma Chemicals Co., USA; 1-palmitoyl-2-oleoyl-*sn*-glycero-3-phosphocholine (POPC) from Avanti Polar Lipids Inc., Alabaster, AL, USA. All chemicals were used without further purification.

2.2. Sample preparation for NMR and DSC

Multilamellar vesicles were prepared using the standard procedure [20]. First the desired quantity of DMPC or DPPC or POPC was dissolved in chloroform. The solvent was evaporated with a stream of nitrogen so as to deposit a lipid film on the walls of the container. The last traces of solvent were removed by vacuum drying for at least 1 h. The film was hydrated with the required amount of a solution of GS-4104 in D_2O (pH 7.2) followed by incubation in a water bath at 50 °C with repeated vortexing. The lipid concentrations were maintained at 100 mM for NMR and 50 mM for DSC experiments. The GS-4104 concentrations were varied from 1 mM to 100 mM for NMR and 0.5 mM to 50 mM for DSC studies. Unilamellar vesicles were prepared by sonicating the above dispersions with a Branson sonicator-450 at 50% duty cycles, till optical clarity was obtained.

GS-4104 is reported to be stable at the temperature and pH used in our experiments [10]. Further assurance of the stability comes from the NMR spectra that have been recorded, which indicate that the molecule is indeed stable and does not degrade under the experimental conditions.

2.3. DSC experiments

DSC measurements were performed using the differential scanning calorimeter VP-DSC (MicroCal, Northampton, MA, USA). The samples were degassed under vacuum before being loaded into the reference and sample cells. A scan rate of 10 °C/h was employed. Data were analyzed with the software ORIGIN provided by MicroCal. All experiments were carried out in the temperature range 20 °C to 60 °C. Repeated scans for the same sample were generally superimposable.

2.4. NMR experiments

NMR experiments were recorded on a BRUKER AVANCE 500 MHz spectrometer. 2D COSY, NOESY and ROESY [21–23] experiments were recorded at 300 K. ^{31}P and ^{13}C NMR experiments were carried out using a relaxation delay of 1 s and with broadband proton decoupling. The NMR data was processed using Topspin 2.1.

2.5. TEM experiments

TEM experiments were performed on a Carl Zeiss Libra 120 EF TEM (Germany) with LaB_6 emitter and 120 kV accelerating voltage. Lipid samples were deposited on Formvar®-carbon coated copper grids (FCF400-Cu, Electron Microscopy Sciences, Hatfield, PA) and allowed to equilibrate. Excess liquid was removed with a filter paper and the grid was air-dried.

2.6. Computational studies

Computational studies were carried out with the modeling package Discovery Studio 2.0 (Accelrys Inc., USA) [24] running on a Red Hat Enterprise Linux WS Workstation. Docking studies were

carried out with GOLD v 3.2 (CCDC, UK) [25] running on a separate Red Hat Enterprise Linux WS Workstation.

2.6.1. Preparation of enzyme and ligand for docking

The crystal structure of the enzyme H5N1-NA in complex with GS-4071 was taken from the protein data bank (PDB code No. 2HU4, H252Y mutant) [15]. The enzyme is an octamer of 8 chains; however for docking studies only the monomeric unit was used. The mutated residue (H252Y) was changed from tyrosine to histidine. All the water molecules were deleted and hydrogens were added at pH 7. The system was refined using the CHARMm forcefield with the backbone atoms tethered by a force constant of 10 kcal/mol/Å, to a gradient of 0.1 kcal/mol/Å.

The structure of GS-4071 was energy minimized using the "Smart Minimizer" method in DS2.0 that performs steepest descents and conjugate gradients with the CHARMm force field to a gradient of 0.01 kcal/mol/Å.

2.6.2. Docking studies

The following parameters in GOLD were permitted to change during the docking runs: (a) the dihedral angles of the inhibitors (b) the inhibitors' ring geometries (flipping ring corners) (c) the dihedral angles of enzyme OH and NH_2 groups and (d) mappings of the H-bonds between the inhibitor and enzyme. At the start of a docking run, all these variables were randomized. Docking was carried out for 20 genetic algorithm (GA) runs, which was found sufficient to reproduce the binding pose of GS-4071 in 2HU4. Most of the other GA parameters like population size and the genetic operators were left at their default values. The binding site was defined as a sphere of 10 Å radius around the inhibitor. The docking protocol was validated by the reproduction of the binding pose of GS-4071 in 2HU4. This protocol was then used to dock the other inhibitors to H5N1, to determine their preferred binding orientations. The docked poses were scored using GoldScore. Hydrogen bonds for all the inhibitors with the amino acid residues of the active site were analyzed. The GOLD fitness function is made up of four components: protein-ligand hydrogen bond energy, protein-ligand van der Waals energy (*external vdw*), ligand internal vdw energy and ligand torsional strain energy. Poses were segregated on the basis of GoldScore.

3. Results and discussion

3.1. Docking

Computational docking is one of the useful methods to investigate molecular interactions. The inhibitors GS-4071, GG-167 and RWJ-270201, DANA, and the endogenous substrate sialic acid were docked into H5N1-NA. The poses of GS-4071 obtained by docking are depicted in Fig. 2 and for the other inhibitors in Fig. 3. The hydrogen bonds formed between the substrate/inhibitors and the enzyme are summarized in Table 1.

It is observed from Table 1 that the number of hydrogen bonds in the case of GS-4071 is smaller compared to the two contemporary drugs GG-167 and RWJ-270201. For GS-4071, the interactions are between the carboxylate group and Arg292, Arg371 and Tyr347; the C=O of the carboxamide group of the drug with Arg152 and the NH_2 group of the drug with Glu119 and Asp151. In case of GG-167, the additional interactions are the guanidino amino group of the drug with Trp178 and Glu227, and the glycerol hydroxyl group of the drug with Glu276. These results indicate that the additional interactions in case of GG-167 provided by the guanidino and glycerol moieties, probably contribute to its lower resistance to NA seen among the currently available drugs. RWJ-270201 also displays H-bond interactions similar to GG-167.

Docking of sialic acid the endogenous substrate shows a binding pattern very similar to the inhibitor GS-4071, except that it does not

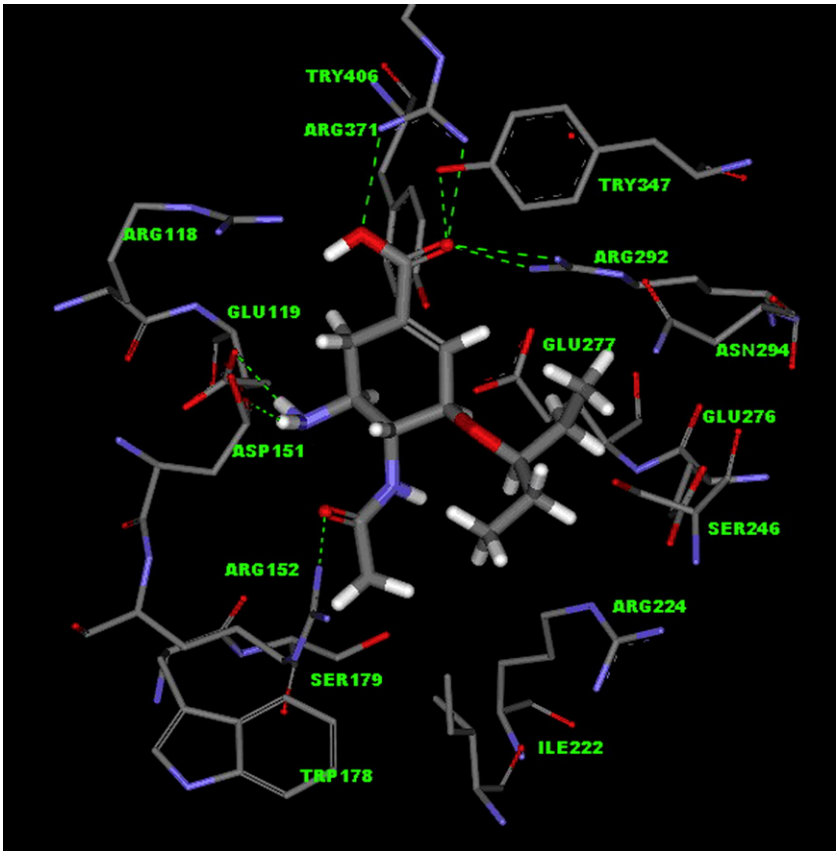

Fig. 2. The most favored pose of oseltamivir carboxylate (GS-4071) in the H5N1-NA active site as seen by docking studies. H-bonds between the drug and the enzyme are indicated.

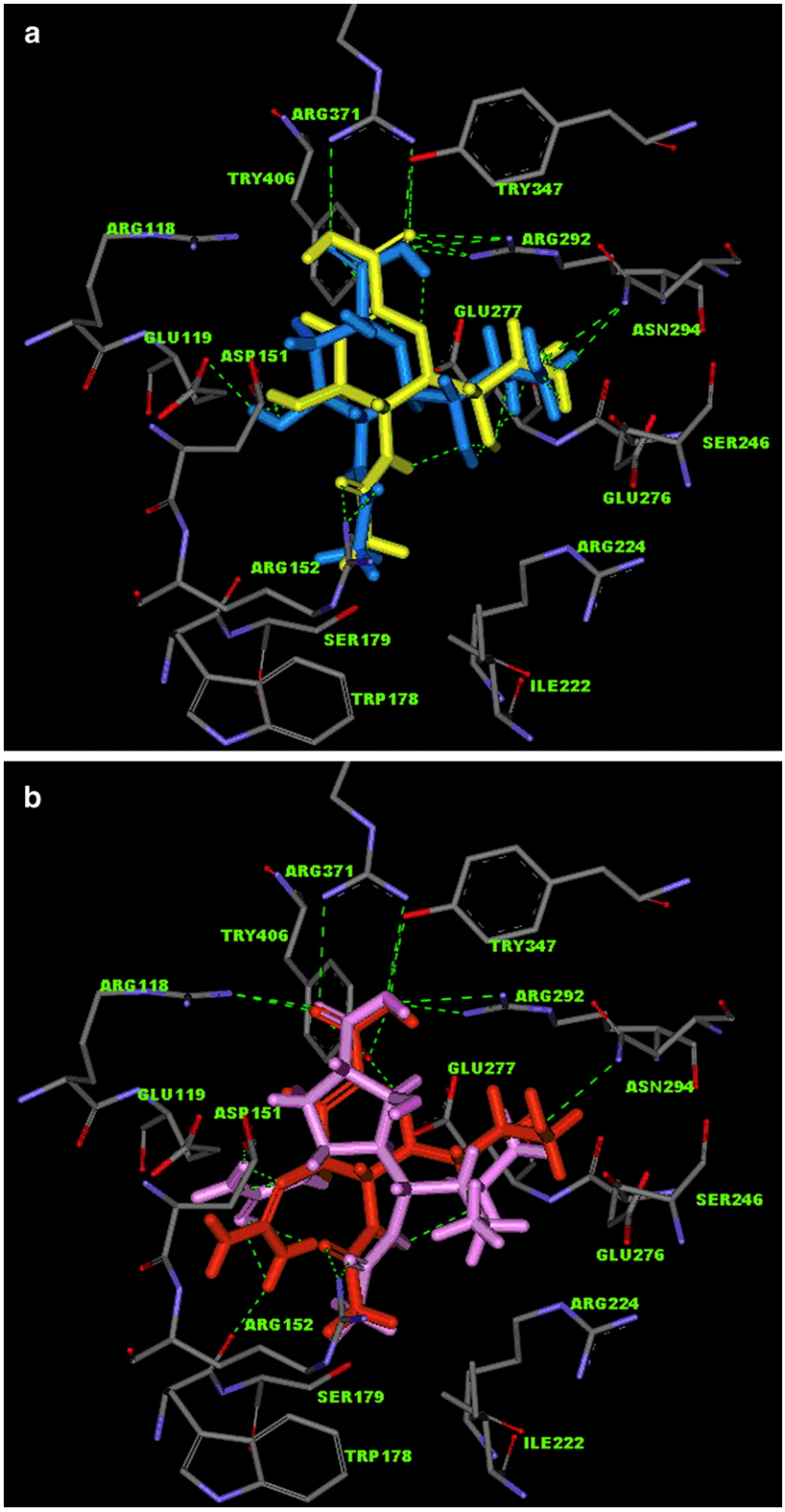

Fig. 3. Favored docking poses of ligands in the H5N1-NA active site. (a) Sialic acid (blue) and DANA (yellow) (b) zanamivir (GG-167, orange) and peramivir (RWJ-270201, pink).

interact with Asp151. DANA on the other hand, shows less hydrogen bonding interactions compared to the other inhibitors. This is also supported by the lack of binding at Asp151 in our docking studies, which probably explains the observed lower activity of DANA compared to the other NA inhibitors [5]. The results correlate with the fact that the lack of a positive charge on sialic acid and DANA (presence of the hydroxyl group instead of an amino/guanidine group) does not facilitate the interaction with Asp151 in these two cases.

Molecular modeling studies reveal that in order to accommodate the hydrophobic side chain of GS-4071 in the active site, the

Table 1
Results of docking studies of oseltamivir (GS-4071) with H5N1-NA

Amino acid residues of H5N1-NA	Oseltamivir GS-4071	Zanamivir GG-167	Ligands peramivir RWJ-270201	DANA	Sialic acid
ARG118		**HO–C**=**O**....HN	**HO–C**=**O**....HN		**HO–C**=**O**....HN
GLU119	**NH$_2$**....O=C				**C–OH**....O=C
ASP151	**NH$_2$**....O=C	**NH$_2$**....O=C	**NH$_2$**....O=C		
ARG152	**HN–C**=**O**....HN	**HN–C**=**O**....HN	**HN–C**=**O**....HN	**HN–C**=**O**....HN	**HN–C**=**O**....HN
TRP178		**NH$_2$**....O=C			
GLU227		**NH$_2$**....O=C	**NH$_2$**....O=C		
GLU276		**C–OH**....O=C			
		C–OH....O=C			
ARG292	**HO–C**=**O**....HN	**HO–C**=**O**....HN	**HO–C**=**O**....HN	**HO–C**=**O**....HN	**HO–C**=**O**....HN
	HO–C=**O**....HN			**HO–C**=**O**....HN	**HO–C**=**O**....HN
TYR347	**HO–C**=**O**....HO	**O**=**C–OH**....HO	**HO**....HO	**HO–C**=**O**....HO	
ARG371	**O**=**C–OH**....HN	**O**=**C–OH**....HN	**O**=**C–OH**....HN	**O**=**C–OH**....HN	**O**=**C–OH**....HN
	HO–C=**O**....HN	**HO–C**=**O**....HN	**HO–C**=**O**....HN	**HO–C**=**O**....HN	**HO–C**=**O**....HN
H bonds	8	11	8	6	7

Atoms involved in hydrogen bonding from ligands (row) to amino acid residues of H5N1-NA (column) are underlined. Last row shows number of hydrogen bonds observed in case of each ligands.

neuraminidase enzyme opens up slightly to create an additional binding pocket [26]. Analysis at the molecular level shows that the amino acid Glu276 must rotate and bond with Arg224 to form such a pocket. Further, the mutations R292K, N294S and H274Y prevent the formation of the Glu276:Arg224 ionic interaction and therefore in such mutants the rotation of Glu276 is inhibited. Consequently the formation of the additional binding pocket is hindered, thereby conferring resistance to GS-4071 [26]. The mutations nonetheless allow the binding of the natural sialic acid substrate, so that the mutated virus can survive and propagate. In contrast, the binding of GG-167 to this pocket does not require any reorientation of amino acids, so these mutated viruses remain sensitive to this drug [26].

Our studies on GG-167 are consistent with the above observations along with an observed additional interaction of its guanidino group with Trp178, Glu227 and Asp151 (Asp151 is part of site 2). At the same time, GS-4071 does not show any interaction with Trp178, Glu227 and Glu276. This indicates that increasing molecular volume of GS-4071, especially around the site-2, may help in more precise binding thereby decreasing the resistance of the enzyme towards the inhibitors.

In view of the above, and based on the docking results for GS-4071 and other inhibitors, we reason that modifying the molecular volume of GS-4071 by extending the length of the C5-amino group, while simultaneously increasing lipophilicity may strengthen the binding interactions and overcome the problem of drug resistance.

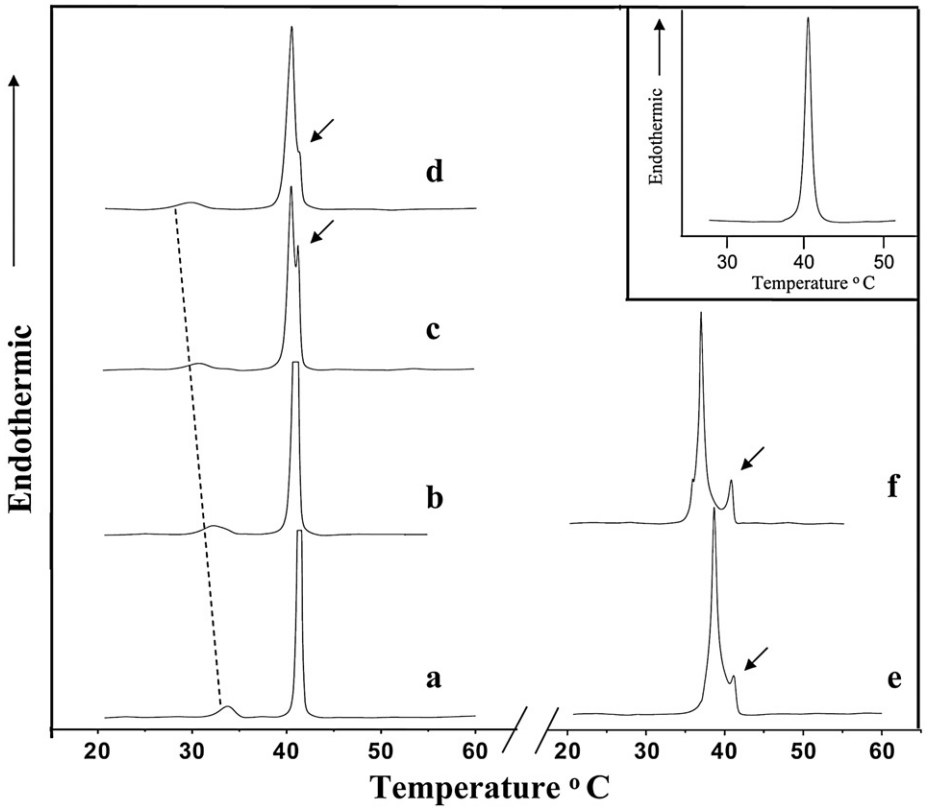

Fig. 4. DSC plots of DPPC (50 mM) with different GS-4104 (as the phosphate salt) to lipid molar ratios (a) 0:100 b) 1:100 c) 1:10 d) 1:5 e) 1:2 f) 1:1 and inset figure 1:1 (GS-4104 here is as the free base *i.e.* without the phosphate group). The arrows indicate the position of the shoulder peaks (T_{m1}) due to the new phase.

Table 2
DSC studies showing the pretransition and main transition temperatures values of DPPC (50 mM) with varying oseltamivir molar ratios

Oseltamivir:DPPC	Pretransition	Main transition (T_m)
0:100	33.74	41.34
1:100	32.40	41.0
1:10	30.96	40.47
1:5	29.88	40.38
1:2	Broad	38.68
1:1	Broad	37.54

3.2. DSC

The thermotropic aspect of drug–lipid interactions can be studied with differential scanning calorimetry (DSC) by examining the changes in the melting point (T_m) and the shape of the DSC trace [27]. During heating, the lipid initially undergoes a pretransition ($L_{\beta'} \rightarrow P_{\beta'}$) from an ordered 'gel' state where the lipids are ordered and tilted ($L_{\beta'}$) to the $P_{\beta'}$ state where the lipids are still ordered and in a gel state but with a minimal tilt. The pretransition occurs before the main transition and is small compared to the main one. During the main transition ($P_{\beta'} \rightarrow L_\alpha$) lipids undergo a change from the ordered state ($P_{\beta'}$) to a 'fluid' disordered state L_α [28,29]. Fig. 4 shows the DSC curves of DPPC incorporated with varying concentrations of GS-4104. It is observed that the multilamellar structure of plain DPPC shows a pretransition or low enthalpy transition at 33.7 °C (Fig. 4), which is an indication of the mobility of the choline part of the polar head of DPPC. The mobility of the alkyl chain is seen in the main transition at 41.3 °C. The effect of incorporation of GS-4104 at different concentrations (from 0.5 mM to 50 mM) into DPPC bilayers is shown in Fig. 4b–f. The addition of GS-4104 causes significant changes in the pretransition as well as in the main phase transition temperature (T_m) of the DPPC bilayers (Table 2). Both the transition temperatures shift to a lower value and the peaks broaden with increasing concentration of the drug. At a drug concentration of as low as 1:100 (drug:lipid molar ratio), the pretransition peak shifts to a lower temperature (32.4 °C) and the main transition peak shifts to 41.0 °C with a symmetrical signal. At higher 1:10 and 1:5 molar ratios the pretransition shifts to 30.9 °C and 29.8 °C respectively, and the main transition peak shifts to 40.4 °C and 40.3 °C respectively. In addition, a shoulder appears at the main transition (T_{m1}) at 41.3 °C and 41.2 °C respectively. At 1:2 molar ratio, the pretransition peak is completely abolished and the main transition shifts to a low of 38.6 °C with a prominent shoulder at 41.1 °C (Fig. 4e). At 1:1 molar ratio, where 50 mM GS-4104 was incorporated into the lipid, a much more pronounced effect is observed. The pretransition peak is completely abolished (broadened nearly to the baseline), the main transition peak shifts to a still lower value (37.5 °C) and the shoulder peak is distinctly converted to an inseparable prominent peak (Fig. 4f). Moreover, the intensity of the new peak corresponding to a new phase increases with increasing drug concentration. The T_m and T_{m1} transitions are observed probably due to the coexistence of GS-4104-rich and GS-4104-poor DPPC domains (phases) within the bilayer.

The presence of coexisting phases indicates phase segregation which may arise from the effect of osmotic stress on DPPC bilayers due to the presence of the phosphate group in GS-4104 [30]. This is supported by studies carried out on modified GS-4104 where the phosphate group has been removed, at 1:1 drug:lipid molar ratio. It is observed that in this case the pretransition peak is abolished, the main transition is broadened and shifted to 38.8 °C. However the shoulder peak which was seen as indicated above (indicative of phase segregation) is absent (Inset Fig. 4) at all concentrations (figure not shown). This indicates that the phosphate group of the GS-4104 is the one interacting with the polar head of the lipid bilayer. In general, the pretransition peak is very sensitive to the presence of impurities and is abolished even at small quantities of impurities [31]. In the present case, however, the pretransition peak

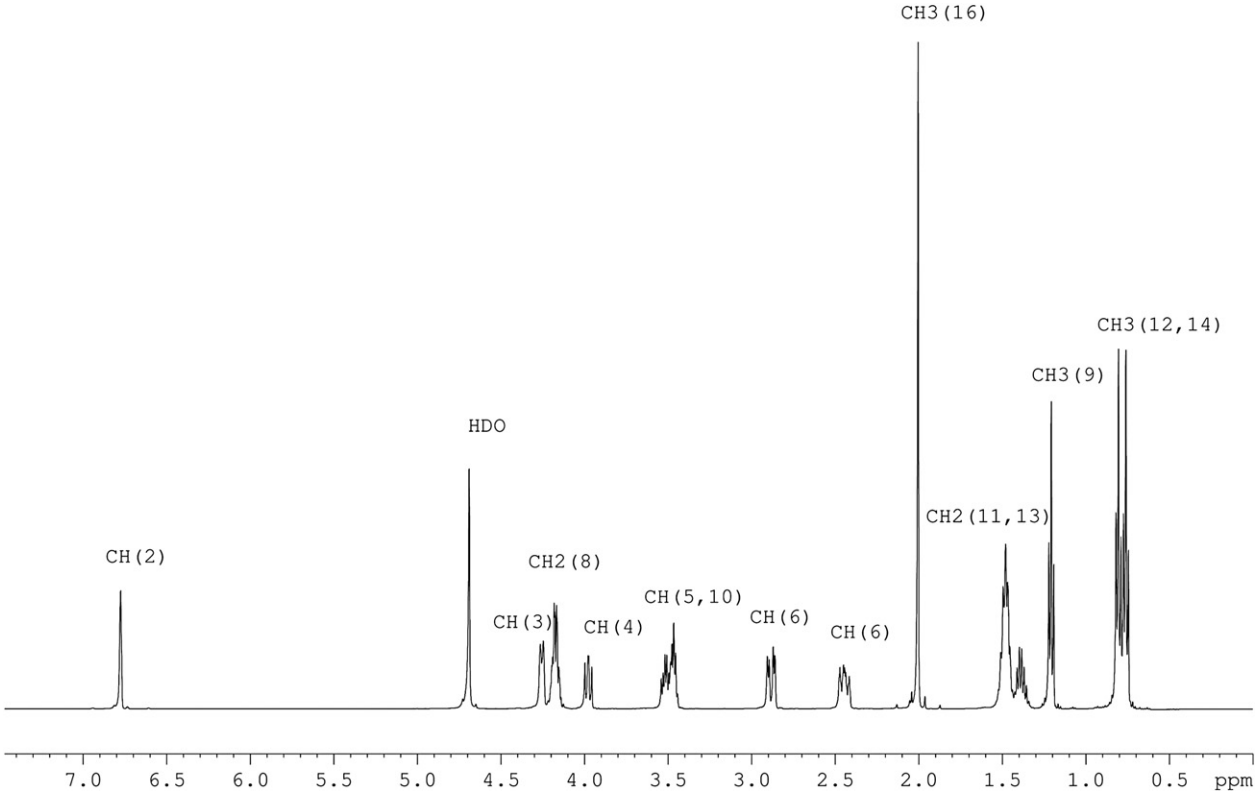

Fig. 5. 500 MHz ^{1}H NMR spectrum of oseltamivir phosphate (GS-4104) in D_2O at 300 K with the resonance assignments. The numbers in the brackets refer to the numbering of the carbon atoms (Fig. 1).

Table 3
^{1}H-NMR chemical shift δ (ppm) of oseltamivir in D_2O

Atoms	δ (ppm)
C(2)H	6.76(s)
C(3)H	4.25(d)
C(8)H_2	4.17(q)
C(4)H	3.97(q)
C(10)H	3.51(m)
C(5)H	3.46(m)
C(6)H_a	2.88(q)
C(6)H_b	2.45(m)
C(16)H_3	2.0(s)
C(11)H_2	1.5(m)
C(13)H_2	1.48(m)
C(9)H_3	1.20(t)
C(12)H_3	0.80(t)
C(14)H_3	0.76(t)

In parenthesis are the multiplicities of the peaks (s)—singlet, (d)—doublet, (t)—triplet, (q)—quadruplet, (m)—multiplet.

does not disappear even at 1:5 drug:lipid molar ratio, although the drug penetrates the lipid bilayer causing the pretransition to shift to a lower temperature. This further suggests that the drug interacts with the head group in such a manner that it stabilizes the membrane architecture to a large extent. Secondly, a decrease in the main transition temperature (~3.8 °C) indicates that the drug imparts a degree of fluidity to the bilayer in order to position itself in the hydrophobic core as well. These observations are further supported by a recent DSC study where both cholesterol and peptide were shown to reduce the T_m markedly and stabilize the fluid phase of the membranes [32].

3.3. NMR

The atoms labels for oseltamivir (GS-4104) as the phosphate salt (Fig. 1a) relate to the ^{1}H and ^{13}C NMR resonances. The ^{1}H NMR spectrum of GS-4104 in D_2O (Fig. 5) has been assigned using the 2D COSY [21] spectrum (Fig. S2) and the chemical shifts are given in Table 3. Comparison of the ^{1}H NMR spectra of DMPC unilamellar vesicles, GS-4104 in D_2O and GS-4104 incorporated into DMPC vesicles indicates no significant changes in the chemical shift of DMPC resonances on incorporation of GS-4104. However, the signals of GS-4104 are broadened to a very large extent on incorporation into DMPC vesicles (Fig. S3), indicating that GS-4104 gets immobilized in the lipid bilayer due to various types of intermolecular interactions. Fig. 6 shows the 2D NOESY [22] spectrum of GS-4104 incorporated into DMPC unilamellar vesicles. Such a spectrum can provide information on intermolecular interactions from the intermolecular NOEs between two molecules. These NOEs arise when the two atoms (within the molecule or from two different molecules) are at a distance ≤5 Å apart. The GS-4104 resonance assignments are indicated in the figure along the F2 dimension. Intermolecular NOEs between the lipid and GS-4104 are indicated in the F1 dimension. These are as follows: C(2)H of GS-4104 with the C(β)H_2 of the lipid head group; C(8)H_2 of GS-4104 with C(β)H of the glycerol backbone and the $N^+(CH_3)_3$ moiety in the head group; C(6)H and C(10)H of GS-4104 with the $(CH_2)_n$ chain of the lipid; C(12,14)H_3 and C(11,13)H_2 of GS-4104 with the $(CH_2)_n$ and the CH_3 groups of the lipid. Other peaks could not be unambiguously assigned due to spectral overlap. Observation of these intermolecular NOEs indicates that GS-4104 uses its hydrophobic chain and the cyclohexene group to bind *via* hydrophobic interactions with the lipid spanning both the head group as well as interior of the lipid bilayer.

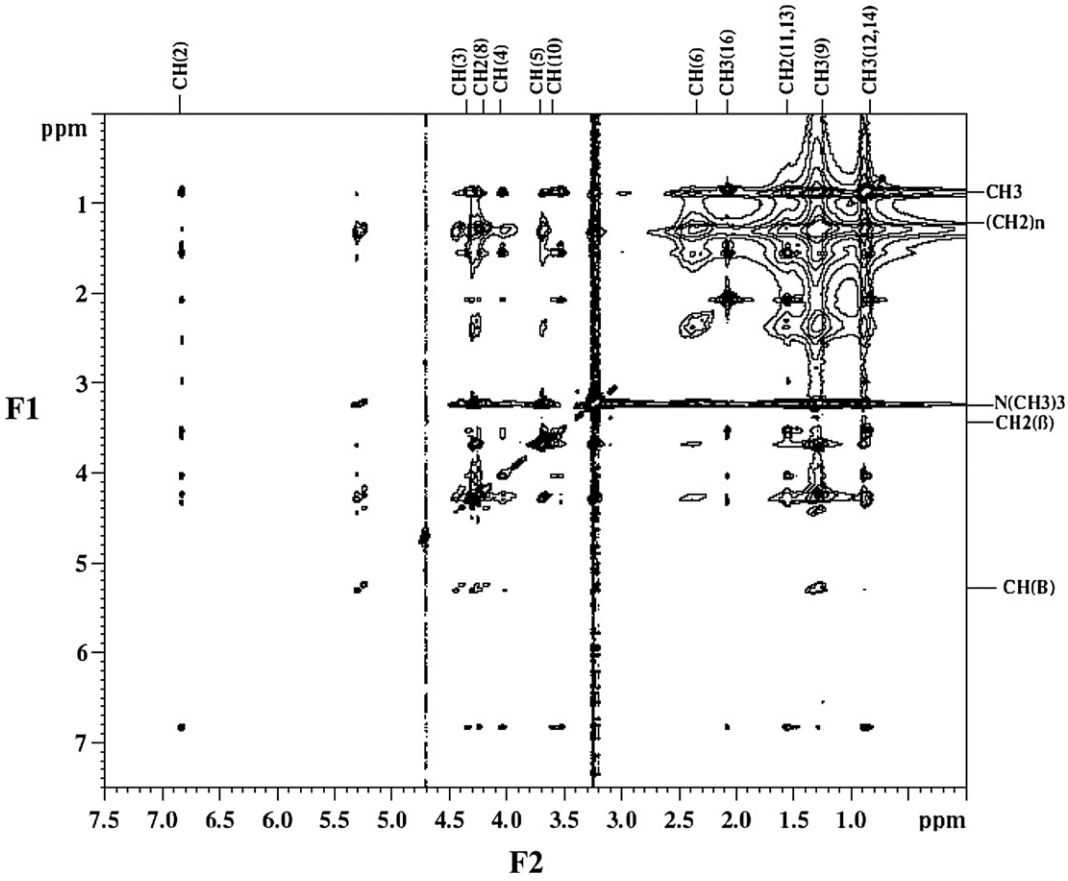

Fig. 6. 2D ^{1}H NOSEY spectrum of DMPC unilamellar vesicles incorporated with oseltamivir phosphate (GS-4104) (1:5 drug:lipid molar ratio). The experiment was carried out at 303 K with a mixing time of 250 ms.

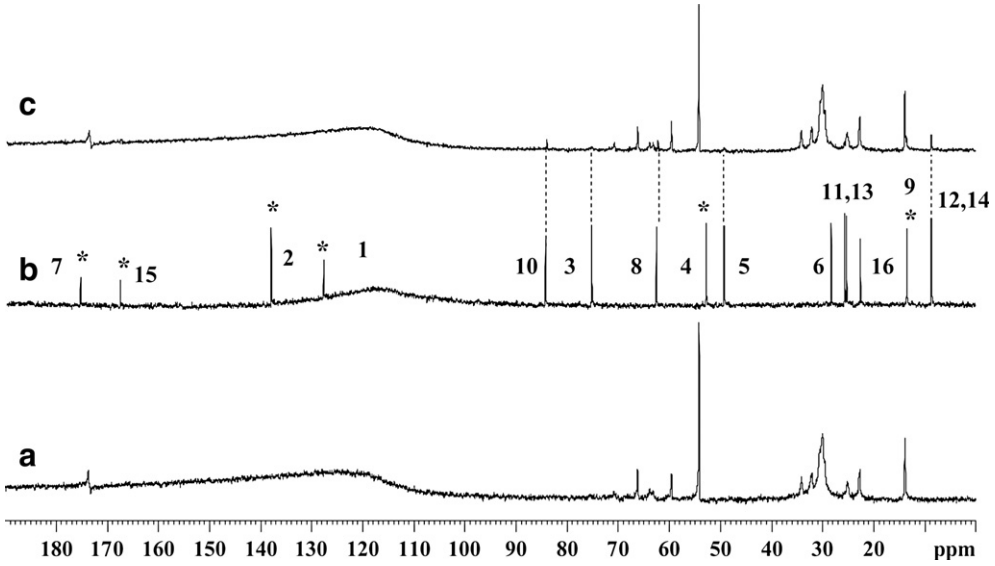

Fig. 7. 125.7 MHz ^{13}C NMR spectra at 303 K. (a) DMPC (50 mM) unilamellar vesicles, (b) oseltamivir phosphate (GS-4104, 10 mM) and (c) DMPC unilamellar vesicles incorporated with oseltamivir phosphate (GS-4104) (1:5 drug:lipid molar ratio). In (b) the asterisk (*) indicates signals of GS-4104 which are broad and beyond detection and dotted lines indicate shift in GS-4104 signals on incorporation into DMPC vesicles.

It was thought that further information on the mode of binding could come from looking at ^{13}C NMR spectra of GS-4104 incorporated into the lipid bilayer (Fig. 7). While the ^{13}C NMR spectrum of DMPC was assigned from the literature [33], GS-4104 peaks were assigned from the DEPT spectrum [34] as well as from the multiplicity pattern of the resonances. The ^{13}C chemical shifts of GS-4104 in D_2O and in lipid bilayers are listed in Table 4. The ^{13}C spectra for unilamellar DMPC vesicles as well as GS-4104 in D_2O are characterized by sharp lines (Fig. 7a and b). On incorporation of GS-4104 into DMPC unilamellar vesicles, the lipid signals continue to remain sharp while the GS-4104 signals show differential broadening. These can be put into three categories: signals that remain sharp but are shifted; those that are broad and shifted, and finally those that are broad beyond detection (Table 4). This differential broadening of the GS-4104 resonances arises because different parts of drug bind to the lipid bilayer with differing affinities.

Due to the broadening of signals it was difficult to measure the spin lattice relaxation time (T_1) and spin–spin relaxation time (T_2), which are measures of the overall tumbling and segmental motions in the molecule. In the fast tumbling range, both T_1 and T_2 are large, of the order of few seconds [35]. The estimates of spin–spin relaxation times (T_2) from the line widths indicate that T_2 values are of the order of 100 ms. The lower values of T_2 indicate that GS-4104 losses its mobility and becomes strongly bound to lipid bilayers resulting in a freezing of its different motions. These results along with the NOEs discussed above indicate that both hydrophilic as well as hydrophobic interactions involve the cyclohexene ring and the hydrophobic chain of GS-4104 with the lipid bilayers.

Membrane fusion is a ubiquitous process in biological systems and involves the union of two opposing bilayers in order to complete processes such as exocytosis or viral infection. A local departure from the bilayer structure must take place in order to allow two lipid membranes to merge into one. Agents known to induce the formation of non-bilayer structures also promote membrane fusion [36–38]. Viral induced cell–cell fusion is known to be inhibited by cyclosporin A, an agent that stabilizes the bilayer phase of membranes [39,40].

The ^{31}P NMR resonance line shape is determined by the chemical shift anisotropy (CSA) of the phosphate group coupled with the molecular motions near the head groups [41]. The shape of the ^{31}P line is used to detect polymorphism in model membranes [42]. In a randomly oriented sample such as DMPC dispersions in the gel phase, the overall rotational rate is slow. One observes a sharp signal at −20 ppm from lipid molecules with their long axis oriented perpendicular to the direction of the magnetic field, while for the parallel alignment of the lipid molecules a broad shoulder appears at 25 ppm (Fig. 8a). A relatively small but sharp peak is observed at 0 ppm due to the formation of a small amount of unilamellar vesicles with a small size that permits fast internal and tumbling motions. The effect of GS-4104 on the ^{31}P NMR line shape of DMPC vesicles was studied as a function of drug concentration (Fig. 8b–d) as well as temperature (Fig. S4). The build up of a sharp peak at zero ppm with increasing GS-4104 concentration is due to the PO_4^- group associated with the drug. The chemical shift anisotropy (CSA) can be measured from the low and high field (the σ_{II} and $\sigma_{\perp}$ components) shoulders of the spectrum. It is seen that with increasing concentration of GS-4104 (1:10 to 1:1 drug:lipid molar ratio) as well with varying temperature, the drug causes a broadening of the low field line (σ_{II} component of the signal). Because of the broad line width of the low field component, the error in the measurement of the CSA is large (Fig. 8, Fig. S4). However, there is a noticeable change (narrowing) in the CSA parameter with increasing temperature (Fig. S4) of the perpendicular

Table 4
^{13}C chemical shifts δ (ppm) of Oseltamivir phosphate in D_2O and in DMPC vesicles (1:5 molar ratio) at 303 K

Atoms	δ (ppm)	In Lipid vesicles δ (ppm)	$\Delta\delta$ (ppm)
C1	127.82	Broad beyond detection	
C2	139.09	Broad beyond detection	
C3	75.24	Broad beyond detection	
C4	52.87	Broad beyond detection	
C5	49.33	49.5 (broad)	0.17
C6	28.33	27.53 (broad)	0.8
C7	175.45	Broad beyond detection	
C8	62.62	62.30 (broad)	0.32
C9	13.50	13.59 (broad)	0.09
C10	84.33	84.01	0.32
C11	25.69	25.80 (broad)	0.11
C12	8.64	8.71	0.07
C13	25.31	25.39 (broad)	0.08
C14	8.74	8.84	0.10
C15	167.62	Broad beyond detection	
C16	22.60	Broad beyond detection	

$\Delta\delta$ (ppm) indicates the difference in the chemical shift from drug in D_2O to drug in DMPC vesicles.

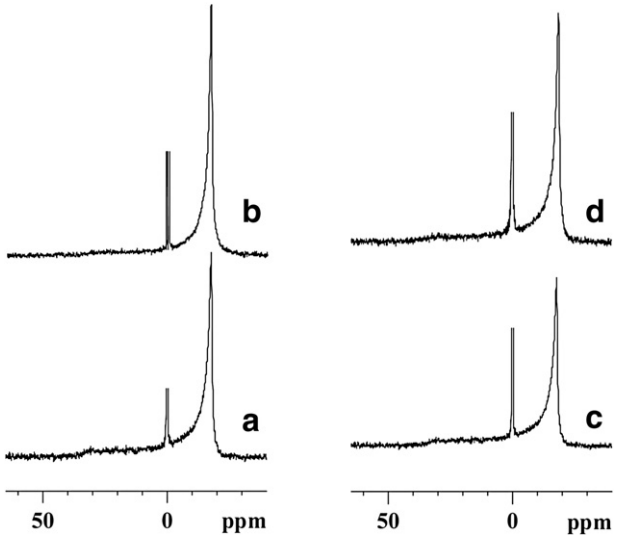

Fig. 8. 202.4 MHz ^{31}P NMR spectra of DMPC (100 mM) incorporated with different concentrations of oseltamivir phosphate (GS-4104) at 303 K. Drug:lipid molar ratios are a) 0:100, b) 1:5, c) 1:2 and d) 1:1.

component at −20 ppm. The narrowing of the signal at −20 ppm may be attributed to motionally averaged isotropic phase above the phase transition temperature. However, the characteristic features of the bilayer (presence of both parallel and perpendicular components) remain unchanged. This indicates that GS-4104 stabilizes the lipid bilayer phase of DMPC [43,44].

Similar concentration and temperature dependence experiments have been carried out with POPC vesicles as well. Fig. 9 shows the ^{31}P NMR spectra of POPC alone and with GS-4104 at a 1:2 drug:lipid molar ratio as a function of temperature. In this case it is observed that there is a partial averaging of the $\sigma_{\perp}$ and σ_{II} components resulting in a reduction in the CSA which is represented by $\Delta\sigma=\sigma_{\perp}-\sigma_{II}$ (inset Fig. 9). The amount by which the CSA is reduced is related to the allowed amplitude of the motion. At lower temperatures (283 K and 288 K) the presence of GS-4104 causes hardly any change in the CSA. However, the reduction in CSA increases with increasing temperature and a maximum decrease in CSA caused by GS-4104 at 308 K is about 1780 Hz as compared to 765 Hz in case of pure POPC. Concentration dependence experiments (carried out at 1:10 and 1:1 drug:lipid ratio) do not show any noticeable change in CSA or line width of the signal (figure not shown).

Studies have shown that stabilization of the membrane by antiviral drugs can play an important role in inhibiting membrane fusion and also antiviral activity [40]. Based on the above observations GS-4104 is likely to be involved in preventing membrane fusion in addition to inhibiting the NA activity.

In order to understand the role of the amide NH and amino NH_2 groups of GS-4104 in interaction with the lipid membrane we have recorded ^{1}H NMR spectra of GS-4104 alone in $CDCl_3$ (in order to avoid NH exchange with D_2O) and titrated with different lipid (DPPC) concentrations (Fig. S5). It is observed that with increasing concentration of lipid, both NH and C5-NH_2 peaks of GS-4104 shift downfield. There is no change in the chemical shift of other resonances. This indicates that probably the NH_2 and NH groups are involved in some sort of hydrogen bonding with the polar head group of the lipid bilayer.

3.4. TEM

TEM has evolved as an important tool to gain new information on the form and structure of liposomes, as well as on the morphological

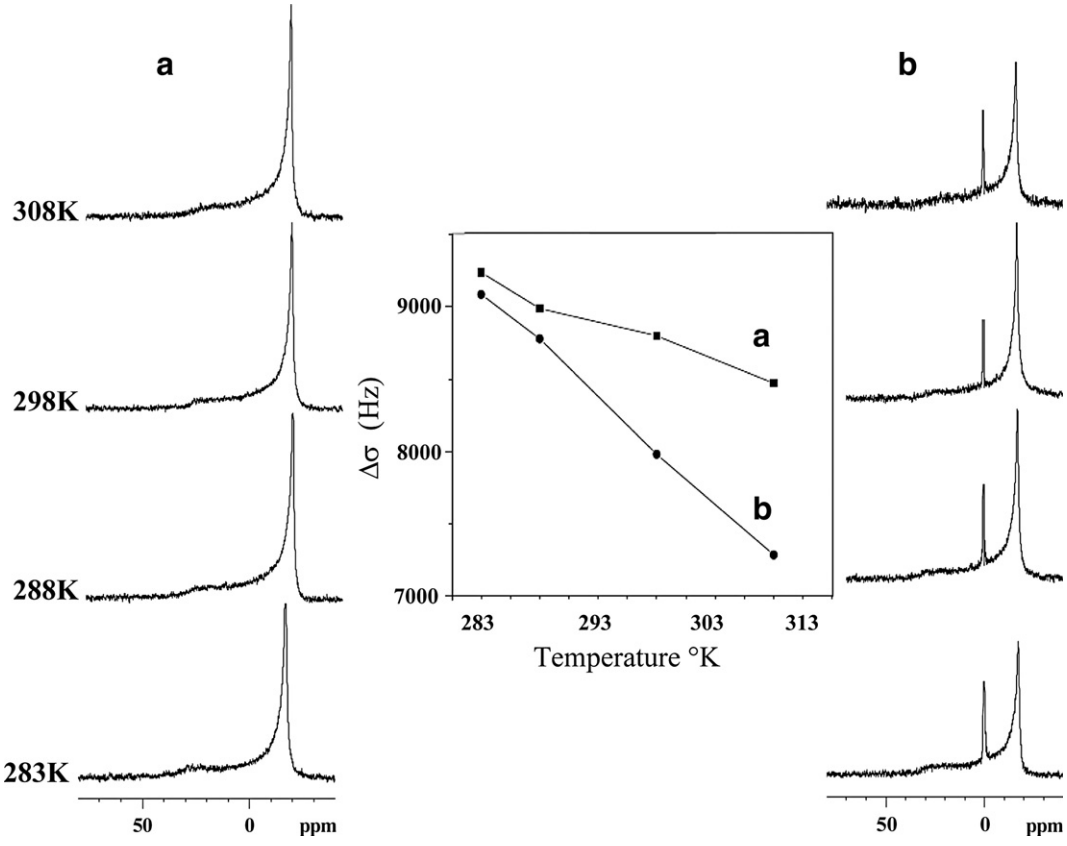

Fig. 9. 202.4 MHz ^{31}P NMR spectra as a function of temperature (a) POPC multilamellar vesicles (b) POPC multilamellar vesicles incorporated with oseltamivir phosphate (GS-4104) at a 1:5 drug:lipid molar ratio. Inset figure shows the change in CSA (Hz) represented by $\Delta\sigma=\sigma_{\perp}-\sigma_{II}$, with temperature.

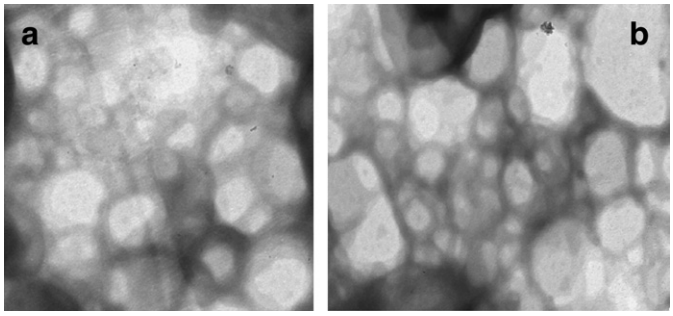

Fig. 10. Transmission electron microscope (TEM) picture of (a) DPPC multilamellar vesicles and (b) vesicles incorporated with oseltamivir in 1:5 drug:lipid ratio.

changes taking place upon interaction with drugs, surfactants, DNA and other polyelectrolytes [45]. As discussed in the Introduction section, NA inhibitors are known to inhibit the binding of HA to its receptor, and thus its ability to promote attachment and fusion of cell membrane to the virus [16,17]. The drug is therefore likely to interfere with cell–cell fusion; through stabilization of the bilayer structure it interferes with the virus entry step. In order to support the stabilization of the lipid bilayer phase by GS-4104 as seen by NMR, we have studied the phase behavior and the aggregate structure of liposomes using TEM. Fig. 10 shows electron micrographs of DPPC dispersions alone and in presence of GS-4104 (1:5 drug:lipid molar ratio). It is observed that pure DPPC dispersions show the characteristic bilayer features of large vesicles (Fig. 10a). On addition of GS-4104 the bilayer characteristics of the lipid dispersions is largely retained and no polymorphism is observed. Moreover, there is a complete absence of any fusion bodies in the micrograph (Fig. 10b). This is in contrast to the studies with the fusogenic drug piroxicam which is seen in TEM micrographs to induce membrane fusion [46] when compared to control samples of DMPC dispersions.

These results thus indicate that GS-4104 binds to the cell membrane in such a way that it stabilizes the bilayer character of the membrane and thus prevents the cell–cell fusion which is an important phenomenon during the viral entry in the host cell [47–49].

4. Conclusions

Oseltamivir—the ethyl ester prodrug (GS-4104) fluidizes the membrane and binds to both the hydrophilic head group (probably involving the amino NH_2 group) and the hydrophobic interior. This may explain the facile transport of the hydrophobic prodrug through the lipid membrane, resulting in its higher absorption from the gut. It also seen to stabilize the bilayer character of the membrane; by which mechanism it prevents membrane fusion of the virus with the cells. Docking studies of oseltamivir (GS-4071) and marketed NA inhibitors with H5N1 indicate the importance of molecular volume at site 2 of the receptor. Therefore, increasing the chain length and lipophilicity may strengthen the binding interactions and overcome the problem of drug resistance. In order to enhance the molecular volume and lipophilicity, introduction of functional groups with proper shape, size and electronic charge are required. This will promote a snug fit to the receptor site and enhance its anti-viral effect. Efforts are on to suitably modify oseltamivir based on these results, with the hope that these modified structures may be able to overcome the problem of the resistance of the mutated enzyme neuraminidase.

Acknowledgements

The authors thank Cipla Ltd. for the gift sample of oseltamivir phosphate. Meena Kanyalkar thanks the Department of Science and Technology, Government of India for funding the computational facilities under SERC-FAST track project (SR/FT/L-24/05). Dr. Krishanu Ray and Ms. Seema Shirolikar at the Cryo TEM facility at TIFR and the National Facility for High Field NMR located at TIFR are gratefully acknowledged.

Appendix A. Supplementary data

Supplementary data associated with this article can be found, in the online version, at doi:10.1016/j.bbamem.2008.11.014.

References

[1] P.M. Colman, W.R. Tulip, J.N. Varghese, P.A. Tulloch, A.T. Baker, W.G. Laver, G.M. Air, R.G. Webster, Three-dimensional structures of influenza virus neuraminidase-antibody complexes, Philos. Trans. R. Soc. Lond. B. Biol. Sci. 323 (1989) 511–518.
[2] J.S. Oxford, P. Novelli, A. Sefton, R. Lambkin, New millennium antivirals against pandemic and epidemic influenza: the neuraminidase inhibitors, Antivir. Chem. Chemother. 13 (2002) 205–217.
[3] P. Palese, K. Jobita, M. Ueda, R.W. Compans, Characterization of temperature sensitive influenza virus mutants defective in neuraminidase, Virology 61 (1974) 397–410.
[4] C. Liu, M.C. Eichelberger, R.W. Compans, G.M. Air, Influenza type A virus neuraminidase does not play a role in viral entry, replication, assembly, or budding, J. Virol. 69 (1995) 1099–1106.
[5] C.U. Kim, W. Lew, M.A. Williams, H. Wu, L. Zhang, X. Chen, P.A. Escarpe, D.B. Mendel, W.G. Laver, R.C. Stevens, Structure–activity relationship studies of novel carbocyclic influenza neuraminidase inhibitors, J. Med. Chem. 41 (1998) 2451–2460.
[6] W. Lew, X. Chen, C.U. Kim, Discovery and development of GS 4104 (oseltamivir): an orally active influenza neuraminidase inhibitor, Curr. Med. Chem. 7 (2000) 663–672.
[7] C.J. Dunn, K.L. Goa, Zanamivir: a review of its use in influenza, Drugs 58 (1999) 761–784.
[8] Y.S. Babu, P. Chand, S. Bantia, P.L. Kotian, A. Dehghani, Y. El-Kattan, T. Lin, T.L. Hutchison, A.J. Elliot, C.D. Parker, S.L. Ananth, L.L. Horn, G.W. Laver, J.A. Montgomery, BCX-1812 (RWJ-270201): discovery of a novel, highly potent, orally active, and selective influenza neuraminidase inhibitor through structure-based drug design, J. Med. Chem. 43 (2000) 3482–3486.
[9] C.U. Kim, W. Lew, M.A. Williams, H. Liu, L. Zhang, S. Swaminathan, N. Bischofberger, M.S. Chen, D.B. Mendel, C.Y. Tai, W.G. Laver, R.C. Stevens, Influenza neuraminidase inhibitors possessing a novel hydrophobic interaction in the enzyme active site: design, synthesis, and structural analysis of carbocyclic sialic acid analogues with potent anti-influenza activity, J. Am. Chem. Soc. 119 (1997) 681–690.
[10] R. Oliyai, L. Yuan, T.C. Dahl, S. Swaminathan, K. Wang, W.A. Lee, Biexponential decomposition of a neuraminidase inhibitor prodrug (GS-4104) in aqueous solution, Pharm. Res. 15 (1998) 1300–1304.
[11] D.B. Mendel, C.Y. Tai, P.A. Escarpe, W. Li, R.W. Sidwell, J.H. Huffman, C. Sweet, K.J. Jakeman, J. Merson, S.A. Lacy, W. Lew, M.A. Williams, L. Zhang, M.S. Chen, N. Bischofberger, C.U. Kim, Oral administration of a prodrug of the influenza virus neuraminidase inhibitor GS 4071 protects mice and ferrets against influenza infection, Antimicrob. Agents Chemother. 42 (1998) 640–646.
[12] W. Li, P.A. Escape, E.J. Eisenberg, K.C. Cundy, C. Sweet, K.J. Jakeman, J. Merson, W. Lew, M. Williams, L. Zhang, C.U. Kim, N. Bischofberger, M.S. Chen, D.B. Mendel, Identification of GS-4104 as an orally bioavailable prodrug of the influenza virus neuraminidase inhibitor GS-4071, Antimicrob. Agents Chemother. 42 (1998) 647–653.
[13] P.M. Colman, P.A. Hoyne, M.C. Lawrence, Sequence and structure alignment of paramyxovirus hemagglutinin-neuraminidase with influenza virus neuraminidase, J. Virol. 67 (1993) 2972–2980.
[14] G.T. Wang, Y. Chen, S. Wang, Design, synthesis, and structural analysis of influenza neuraminidase inhibitors containing pyrrolidine cores, J. Med. Chem. 44 (2001) 1192–1201.
[15] R.J. Russell, L.F. Haire, D.J. Stevens, P.J. Collins, Y.P. Lin, G.M. Blackburn, A.J. Hay, S.J. Gamblin, J.J. Skehel, The structure of H5N1 avian influenza neuraminidase suggests new opportunities for drug design, Nature 443 (2006) 45–49.
[16] O. Greengard, N. Poltoratskaia, E. Leikina, J. Zimmerberg, A. Moscona, The anti-influenza virus agent 4-GU-DANA (zanamivir) inhibits cell fusion mediated by human parainfluenza virus and influenza virus HA, J. Virology (2000) 11108–11114.
[17] M. Porotto, M. Murrell, O. Greengard, M.C. Lawerence, J.L. Mckimm-Breschkin, A. Moscona, Inhibition of parainfluenza virus type 3 and Newcastle disease virus hemagglutinin-neuraminidase receptor binding: effect of receptor avidity and steric hindrance at the inhibitor binding sites, J. Virol. 78 (2004) 13911–13919.
[18] J.S. Santos, D. Lee, A. Ramamoorthy, Effects of antidepressants on the conformation of phospholipid headgroups studied by solid-state NMR, Magn. Reson. Chem. 42 (2004) 105–114.
[19] A. Ramamoorthy, S. Thennarasu, D. Lee, A. Tan, L. Maloy, Solid-state NMR investigation of the membrane-disrupting mechanism of antimicrobial peptides MSI-78 and MSI-594 derived from magainin 2 and melittin, Biophys. J. 91 (2006) 206–216.
[20] R.D. Kornberg, H.M. McConnel, Inside–outside transitions of phospholipids in vesicle membranes, Biochemistry 10 (1971) 1111–1120.

[21] W.P. Aue, E. Bartholdi, R.R. Ernst, Two-dimensional spectroscopy. Application to nuclear magnetic resonance, J. Chem. Phys. 64 (1976) 2229–2248.
[22] J. Jeener, B.H. Meier, P. Bachmann, R.R. Ernst, Investigation of exchange processes by two-dimensional NMR spectroscopy, J. Chem. Phys. 71 (1979) 4546–4553.
[23] A.A. Bothner-By, R.L. Stephens, J. Lee, C.D. Waren, R.W. Jeanloz, Structure determination of a tetrasaccharide: transient nuclear Overhauser effects in the rotating frame, J. Am. Chem. Soc. 106 (1984) 811–813.
[24] Discovery Studio version 2.0, Accelrys Inc., USA.
[25] GOLD 3.0.1 CCDC Ltd., UK.
[26] M.D. de Jong, T.T. Tran, H.K. Truong, M.H. Vo, G.J. Smith, V.C. Nguyen, V.C. Bach, T.Q. Phan, Q.H. Do, Y. Guan, J.S. Peiris, T.H. Tran, J. Farrar, Oseltamivir resistance during treatment of influenza A (H5N1) infection, N. Engl. J. Med. 353 (2005) 2667–2672.
[27] M.P. Lambros, E. Sheu, J.S. Lin, H.A. Pereira, Interaction of a synthetic peptide based on the neutrophil-derived antimicrobial protein CAP37 with dipalmitoyl-phosphatidylcholine membranes, Biochim. Biophys. Acta 1329 (1997) 285–290.
[28] M.J. Janiak, D.M. Small, G.G. Shipley, Nature of the thermal pretransition of synthetic phospholipids: dimyristoyl- and dipalmitoyllecithin, Biochemistry 15 (1976) 4575–4580.
[29] M.J. Ruocco, G.G. Shipley, Characterization of the subtransduction of hydrated dipalmitoylphosphatidylcholine bilayers, Biochim. Biophys. Acta 691 (1982) 309–320.
[30] W.R. Perkins, X. Li, J.L. Slater, P.A. Harman, P.L. Ahl, S.R. Minchey, S.M. Gruner, A.S. Janoff, Solute-induced shift of phase transition temperature in Di-saturated PC liposomes: adoption of ripple phase creates osmotic stress, Biochim. Biophys. Acta 1327 (1997) 41–51.
[31] R.N. McElhaney, Differential scanning calorimetric studies of lipid–protein interactions in model membrane systems, Biochim. Biophys. Acta 864 (1986) 361–421.
[32] R.F. Epand, A. Ramamoorthy, R.M. Epand, Membrane lipid composition and the interaction of pardaxin: the role of cholesterol, Prot. Peptide Lett. 13 (2006) 1–5.
[33] J.M. Neumann, A. Zachowski, S. Tran-Dinh, P.F. Devaux, High resolution proton magnetic resonance of sonicated phospholipids, Eur. Biophys J. 11 (1985) 219–223.
[34] M.R. Bendall, D.T. Pegg, Complete accurate editing of decoupled ^{13}C spectra using DEPT, J. Mag. Res. 53 (1983) 272–296.
[35] D.A. Keire, M. Kobayashi, The orientation and dynamics of substance P in lipid environments, Protein Sci. 7 (1998) 2438–2450.
[36] H. Ellens, J. Bentz, F.C. Szoka, Fusion of phosphatidylethanolamine-containing liposomes and mechanism of the L_a–H_{II} phase transition, Biochemistry 25 (1986) 4141–4147.
[37] P.R. Cullis, M.J. Hope, C.P.S. Tilcock, Lipid polymorphism and the role of lipids in membranes, Chem. Phys. Lipids 40 (1986) 127–144.
[38] N. Duzgunes, D.B. Roodyn (Eds.), Subcellular Biochemistry, Plenum Press, New York, 1985, pp. 195–286.
[39] R.C. McKenzie, R.M. Epand, D.C. Johnson, Cyclosporine A inhibits herpes simplex virus-induced cell fusion but not virus penetration into cells, Virology 159 (1987) 1–9.
[40] R.M. Epand, R.F. Epand, R.C. McKenzie, Effects of viral chemotherapeutic agents on membrane properties. Studies of cyclosporin A, benzyloxycarbonyl-D-Phe-L-Phe-Gly and amantadine, J. Biol. Chem. 262 (1987) 1526–1529.
[41] S. Srivastava, R.S. Phadke, G. Govil, Role of tryptophan in inducing polymorphic phase formation in lipid dispersion, Ind. J. Biochem. Biophys. 25 (1988) 283–286.
[42] K.V. Chary, G. Govil, NMR in Biological Systems, from Molecules to Humans, Springer, The Netherlands, 2008, pp. 291–315.
[43] S. Thennarasu, D. Lee, A. Poona, K.E. Kawulka, John C. Vederas, A. Ramamoorthya, Membrane permeabilization, orientation, and antimicrobial mechanism of subtilosin A, Chem. Phys. Lipids 137 (2005) 38–51.
[44] A. Ramamoorthy, S. Thennarasu, A. Tan, D. Lee, C. Clayberger, A.M. Krensky, Cell selectivity correlates with membrane-specific interactions: a case study on the antimicrobial peptide G15 derived from granulysin, Biochim. Biophys. Acta 1758 (2006) 154–163.
[45] M. Almgren, K. Edwards, G. Karlsson, Cryo transmission electron microscopy of liposomes and related structures, Colloids Surf., A Physicochem. Eng. Asp. 174 (2000) 3–21.
[46] H. Chakraborty, P.K. Chakraborty, S. Raha, P.C. Mandal, M. Sarkar, Interaction of piroxicam with mitochondrial membrane and cytochrome *c*, Biochim. Biophys. Acta 1768 (2007) 1138–1146.
[47] A. Kohn, Permeability to inhibitors of protein synthesis in virus infected cells, Adv. Viral Res. 24 (1979) 223–276.
[48] J. White, M. Keilian, A. Helenius, Low pH deforms the influenza virus envelope, Q. Rev. Biophys. 16 (1983) 151–195.
[49] J.D.E. Young, G.P.H. Young, Z.A. Cohn, J. Lenard, Mutational analysis of receptor interaction and membrane fusion activity of sindbis virus, Virology 128 (1983) 186–194.